Received: 3 March 2021 | Revised: 2 May 2021 | Accepted: 10 May 2021

DOI: 10.1002/jor.25102

RESEARCH ARTICLE

Journal of Orthopaedic Research®

Differential effects of anti-RANKL monoclonal antibody and zoledronic acid on necrotic bone in a murine model of *Staphylococcus aureus*-induced osteomyelitis

Hideyuki Kobayashi | Ryo Fujita | Shigeto Hiratsuka | Tomohiro Shimizu | Dai Sato | Hiroki Hamano | Norimasa Iwasaki | Masahiko Takahata

Department of Orthopaedic Surgery, Graduate School of Medicine, Hokkaido University, Sapporo, Japan

Correspondence
Masahiko Takahata, Department of Orthopaedic Surgery, Graduate School of Medicine, Hokkaido University, Kita-15 Nishi-7, Kita-ku, Sapporo 060-8638, Japan.
Email: takamasa@med.hokudai.ac.jp

Funding information
Japan Society for the Promotion of Science (JSPS) Grants-in-Aid for Scientific Research (KAKENHI), Grant/Award Number: JP17H04309

Abstract

Osteomyelitis is characterized by progressive inflammatory bone destruction accompanied by severe pain and disability. However, with the exception of antibiotic therapies, there is no established therapy to protect the bone from infectious osteolysis. The anti-receptor activator of nuclear factor-kB ligand (RANKL) monoclonal antibody (anti-RANKL Ab) is a potential drug based on its proven effectiveness in preventing joint bone erosion in rheumatoid arthritis; however, the efficacy and adverse effects of anti-RANKL Ab in osteomyelitis remain to be investigated. In this study, we investigated the effects of anti-mouse RANKL Ab on acute osteomyelitis and compared them with those of zoledronic acid (ZA) using a murine model. Mice were inoculated with bioluminescent *Staphylococcus aureus* (Xen 29) on their left femur and then treated with ZA, anti-RANKL Ab, or phosphate-buffered saline as control. A 21-day longitudinal observational study using micro-computed tomography showed that both anti-RANKL Ab and ZA had an osteoprotective effect against infectious osteolysis. However, it was also demonstrated through bioluminescence imaging that ZA delayed the spontaneous reduction of bacterial load and through histology that it increased the amount of necrotic bone, while anti-RANKL Ab did not. Findings from histopathological and in vitro studies suggest that an intense inflammatory response around the necrotic bone could induce osteoclasts in a RANKL-independent manner, leading to the removal of necrotic bone, even after administration of the anti-RANKL Ab therapy. Collectively, anti-RANKL Ab may exert an osteoprotective effect without hampering the removal of the necrotic bone, which serves as a nidus for infection in osteomyelitis.

KEYWORDS

antiresorptive therapy, inflammatory bone destruction, necrotic bone, osteoprotective effect, pyogenic osteomyelitis

1 | INTRODUCTION

Osteomyelitis is a bacterial infection of the bone and bone marrow. One hallmark of this disease is rapid bone destruction leading to pathological fracture and paralysis. Bacterial infections can usually be controlled by antibiotics and debridement of the infected bone.[1] However, a cumbersome problem in this disease is that once a large bone defect develops by osteolysis, it requires several months either to regenerate the bone or for additional bone reconstruction surgery, resulting in prolonged hospital stays and increased medical costs.[2–4] Therefore, effective adjuvant therapy is needed to prevent the osteolysis associated with osteomyelitis.

Staphylococcus aureus is the most common causative agent of osteomyelitis.[5] *S. aureus* surface-associated material (SAM) and inflammatory cytokines,[6,7] such as tumor necrosis factor-α (TNF-α), interleukin-1 (IL-1), and IL-6, induced by staphylococcal infection of the bone stimulate osteoclast formation and resorption[6,8,9] resulting in rapid bone destruction. To control the pathological bone resorption in osteomyelitis, anti-resorptive agents, such as bisphosphonates (BPs) and denosumab, a human anti-receptor activator of nuclear factor-kB ligand (RANKL) monoclonal antibody, are expected to be effective based on their proven effectiveness in suppressing the joint bone erosion associated with rheumatoid arthritis.[10,11] However, earlier studies have demonstrated that BPs increase the amount of necrotic bone, which harbors bacteria, in murine models of osteomyelitis.[12,13] Thus, it is believed that patients with osteomyelitis would not benefit from antiresorptive therapies.

However, it is unclear whether an anti-RANKL monoclonal antibody (anti-RANKL Ab) has effects on osteomyelitis that are similar to BPs because these two drugs have different mechanisms of action. BPs bind to bone minerals and are taken up by osteoclasts, inhibiting the bone resorption activity of osteoclasts or causing osteoclast cell death by apoptosis.[14] In contrast, the anti-RANKL Ab inhibits osteoclast differentiation, function, and survival by preventing RANKL–receptor activator of nuclear factor-kB (RANK) binding.[15] Given that SAM, IL-1, IL-6, and TNF-α can induce osteoclasts in the absence of RANKL,[6,16–18] an anti-RANKL Ab therapy may be less effective in suppressing osteolysis but may have an advantage in removing necrotic bone as compared to BPs.

In the current study, we compared the effects of an anti-RANKL Ab on osteomyelitis with those of a BP using a murine model of *S. aureus*-induced acute osteomyelitis.

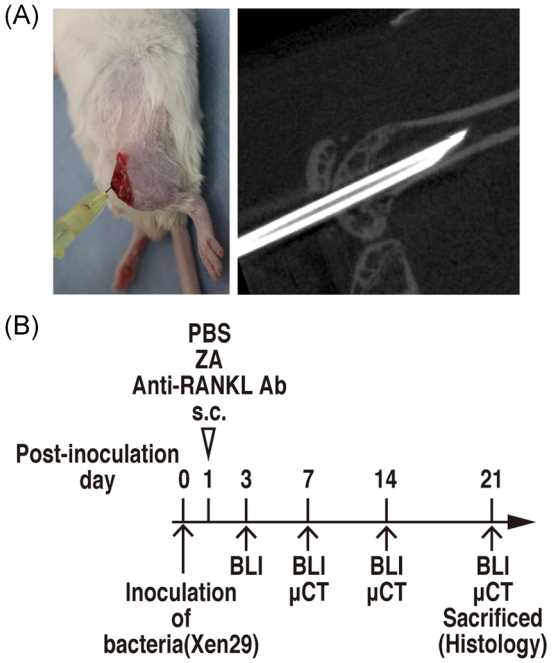

FIGURE 1 Experimental protocol. (A) Representative images of the bacterial inoculation site. Xen 29 were inoculated at a point 6–8 mm from the femoral articular surface. (B) Experimental treatment and evaluation schedule of the mice after Xen 29 inoculation in the left femur. Anti-RANKL Ab, anti-mouse RANKL monoclonal antibody; ZA, zoledronic acid [Color figure can be viewed at wileyonlinelibrary.com]

2 | METHODS

2.1 | Murine *S. aureus*-induced acute osteomyelitis model

All animal studies were performed in accordance with protocols approved by the Institutional Committee on Animal Resources. Male BALB/c mice (12 weeks old; CLEA Japan Inc.) were used in this study. The mice were maintained under a 12-h light/dark cycle with free access to food and water. The light-producing microorganism, *S. aureus* ATCC 12600 (Xen 29), was purchased from Perkin Elmer Inc. (Waltham). We generated an *S. aureus*-induced acute osteomyelitis mouse model in accordance with the protocol reported by Funao et al.[19] Briefly, mice were anesthetized with an intraperitoneal injection of ketamine (95 mg/kg) and medetomidine (0.5 mg/kg). The distal end of the left femur was exposed through lateral parapatellar arthrotomy with medial displacement of the quadriceps-patellar complex. The fossa intercondyloid was perforated using a 23-gauge needle. Then, Xen 29 (1×10^8 colony-forming units) were inoculated into the medial cavity of the femur using a Hamilton syringe and a 27-gauge needle (Figure 1A). The hole was closed with bone wax, and the muscle and skin were closed using sutures. To terminate the anesthesia, the mice were injected intraperitoneally with atipamezole (2.5 mg/kg).

2.2 | Antiresorptive therapies

Mice were randomized into the following three groups with eight mice per group: a control (Ctl) group, a zoledronic acid (ZA) group, and an anti-RANKL monoclonal antibody (anti-RANKL Ab) group. The Ctl group mice were administered phosphate-buffered saline (PBS). ZA (Novartis Pharma) was administered to mice at a dosage of 100 mg/kg, while mice were administered an anti-mouse RANKL monoclonal antibody (OYC1; Oriental Yeast) at 5 mg/kg. The dosages

of ZA and anti-RANKL Ab were determined based on previous studies.[20,21] Mice in all groups were injected subcutaneously a day after surgery (Figure 1B).

2.3 | Noninvasive monitoring of infection by bioluminescence imaging

To assess the time course of infection, bacterial bioluminescent signals were analyzed using a Caliper LS-IVIS imaging system Lumina II (Summit Pharma. Int Co.). The mice were anesthetized as mentioned above, placed on their backs, and imaged for 1 min. To quantify bacterial luminescence, regions of interest were defined in the inoculated area. Photon emissions of the bacterial bioluminescent signal were captured, converted to false-color photon-count images, and quantified using Living Image software (version 4.3; Caliper LS Co.). The bacterial photon signal was expressed as the total flux (photons/s). Bioluminescence imaging (BLI) was performed on Days 3, 7, 14, and 21 postinfection.

2.4 | Longitudinal evaluation of osteolysis by microcomputed tomography

The left femora were scanned individually using micro-computed tomography (CT) (R_mCT2; Rigaku) at 10 μm isotropic resolution. Micro-CT was performed on Days 7, 14, and 21 under anesthesia. The degree of bone-destructive lesions in each group of mice was semiquantified using a subcomponent of the Mirels' score.[22] Measurements were performed using TRI/3D-BON software (Ratoc System Engineering Co.). A 6000-μm area of interest from 600 slices encompassing the region of the distal metaphysis starting from the growth plate was used to assess bone morphology on Day 21. The following indices were calculated: bone mineral content/tissue volume (BMC/TV), trabecular bone volume/tissue volume (BV/TV), and cortical bone volume (Ct.V).

2.5 | Histopathological evaluation

The left femurs were decalcified with 5% ethylenediaminetetraacetic acid-2Na and then embedded in paraffin. Deparaffinized sagittal femur sections were stained with hematoxylin and eosin stain. The ratio of empty lacunae was defined as the ratio of empty to occupied osteocytic lacunae within a 6000 μm area around the inoculation site. The sections were also stained with Gram's stain to evaluate the presence of bacteria. The number of gram-positive cocci was assessed by a semiquantitative method as follows: grade 1+ = rare (bacteria <1/oil immersion field), 2+ = few (bacteria = 2–10/oil immersion field), 3+ = moderate (bacteria = 11–50/oil immersion field), 4+ = many (bacteria >50/oil immersion field).[23] To observe osteoclasts, the sections were stained with tartrate-resistant acid phosphatase (TRAP) and counterstained with methyl green. Images were obtained using a BX53 microscope (Olympus), and histomorphometric measurements were performed using ImageJ software (NIH). The following indices were calculated: osteoclast number per bone surface (N.Oc/BS), osteoclast surface (Oc.S/BS), and eroded surface (ES/BS).

2.6 | In vitro osteoclastogenesis assay

Cells were cultured at 37°C in a humidified incubator with an atmosphere of 5% CO_2. Bone marrow macrophages (BMMs) were collected as previously described.[24] Briefly, bone marrow cells were obtained from the femurs and tibias of 7–9-week-old male mice. After removing the red blood cells, marrow cells were cultured in a suspension culture dish in the presence of 50 ng/ml human macrophage colony-stimulating factor (M-CSF; Peprotech). After 3 days of culture, the cells were washed to remove nonadherent cells, and the adherent cells were harvested as BMMs. Bone marrow stromal cells (BMSCs) were isolated as previously described.[25] Bone marrow cells, which were obtained from the femora and tibiae of 7–9-week-old male mice, were cultured on plastic dishes. After 2 days, nonadherent cells were removed, and adherent cells were used as BMSCs.

Cocultures of BMMs and BMSCs were prepared by plating BMMs and BMSCs at a 1:1 ratio (4×10^4 cells/well in a 48-well plate) in a medium containing 10 nM 1,25-dihydroxyvitamin D_3 (Sigma-Aldrich) and 30 ng/ml M-CSF, with culturing for 5 days to generate osteoclasts. To simulate inflammatory conditions, 10 ng/ml IL-1β (BioLegend) and 10 ng/ml TNF-α (BioLegend) were added to the medium. Monocultures of BMMs (4×10^4 cells/well in 48-well plates) were cultured with 30 ng/ml M-CSF, 10 ng/ml IL-1β, and 10 ng/ml TNF-α for 5 days to generate osteoclasts. PBS as a control, 1 μM ZA, and 1 μg/ml anti-RANKL Ab were administered to assess the therapeutic effects. The doses of ZA and anti-RANKL Ab were determined based on previous reports.[21,26]

2.7 | Statistical analysis

A two-way repeated analysis of variance with Turkey's multiple comparison test was performed to compare longitudinal analysis data after log transformation for non-normally distributed data. A one-way analysis of variance with Tukey's multiple comparison test was performed to compare continuous data. We used a Kruskal–Wallis test with Dunn's multiple comparison test to compare semiquantitative data. All data are expressed as the mean ± *SEM*. Statistical significance was set at $p < .05$.

3 | RESULTS

3.1 | Bone-protective effect of antiresorptive agents against osteomyelitis

To assess whether antiresorptive agents had an osteoprotective effect against osteolysis in osteomyelitis, we longitudinally analyzed

bone destruction in infected femora using micro-CT images. The reconstructed micro-CT images showed that both the anti-RANKL Ab and ZA suppressed the progression of osteolysis (Figure 2A). According to the Mirels scoring system for evaluating the extent of osteolysis, the anti-RANKL Ab and ZA groups had significantly lower scores for osteolytic lesion size than did the Ctl group on Day 14 (ZA vs. Ctl: $p = .0247$) and Day 21 (ZA vs. Ctl: $p = .0351$; anti-RANKL vs. Ctl: $p = .0351$) (Figure 2B). On Day 21, the BMC/TV was significantly higher in the anti-RANKL Ab and ZA groups than in the Ctl group (ZA vs. Ctl: $p = .0003$; anti-RANKL vs. Ctl: $p = .0023$). BV/TV was significantly higher in the ZA group than in the Ctl group (ZA vs. Ctl: $p = .0092$). Despite trends suggesting an increase in BV/TV in the anti-RANKL Ab group, the effect of the anti-RANKL Ab was not statistically significant (anti-RANKL Ab vs. Ctl: $p = .1689$). There were no significant differences in Ct.V among the three groups (ZA vs. Ctl: $p = .0629$; anti-RANKL Ab vs. Ctl: $p = .8130$) (Figure 2C). However, Ct.V includes reactive newly formed bone as well as original bone in the distal metaphyseal region where the infection was acquired. Although the difference in the effect of anti-resorptive therapies on reactive bone formation in a region with destructive bone is of great interest, we could not distinguish newly formed bone from original bone by micro-CT because there is a mixture of reactive bone and destroyed original bone.

To address the question as to whether ZA and the anti-RANKL Ab exert protective effects on systemic bone loss in the mouse model of osteomyelitis, we scanned the contralateral noninfected femora from the Ctl, ZA, and anti-RANKL Ab groups using micro-CT and measured the BMC/TV and BV/TV at the distal metaphyseal region. The BMC/TV and BV/TV in the contralateral femur were significantly higher in the anti-RANKL Ab and ZA groups than in the Ctl group and were comparable between the ZA and anti-RANKL Ab groups (Figure 2D,E), suggesting that anti-RANKL Ab and ZA are equally effective in preventing systemic bone loss in osteomyelitis.

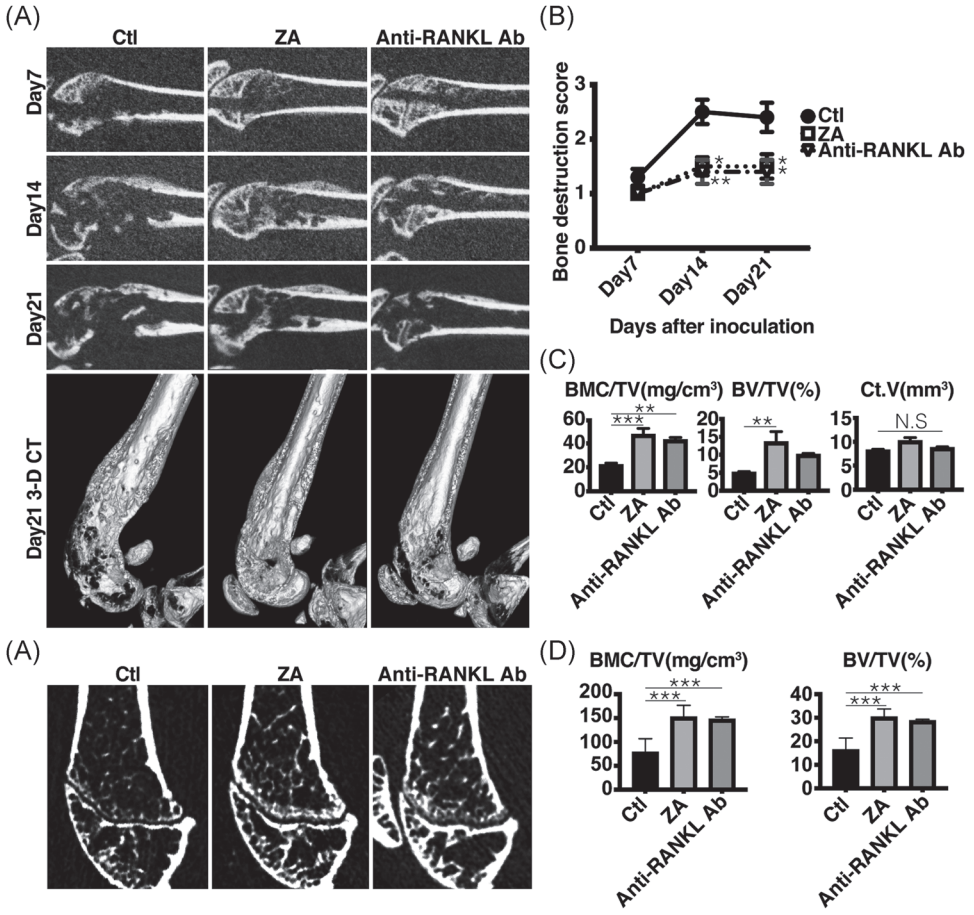

FIGURE 2 Longitudinal radiographical assessment of the osteolytic lesions of the femur in a murine model of osteomyelitis using micro-CT imaging. (A) Representative sagittal reconstruction images and 3D rendering images of the distal femur from each treatment group at different time points (the same animal's femur was used for the longitudinal series). Ctl: control group; ZA: zoledronic acid treatment group; Anti-RANKL Ab: anti-mouse RANKL monoclonal antibody treatment group. (B) The degree of bone-destruction lesions in each group ($n = 8$) of mice was semiquantified using a subcomponent of Mirels' score at different time points. (C) Bone mineral content/total volume of interest (BMC/TV), trabecular bone volume/tissue volume (BV/TV), and cortical bone volume (Ct.V) of the distal metaphysis of the femur. (D) Representative sagittal reconstruction images of the distal contralateral noninfected femur from each treatment group. (E) BMC/TV and BV/TV of the distal metaphysis of the noninfected distal femur. Values shown are mean ± *SEM* (*$p < .05$; **$p < .01$; vs. Ctl). CT, computed tomography; Ctl, control; RANKL, receptor activator of nuclear factor-kB ligand

3.2 | Delayed attenuation of bacterial load in the infected femur of ZA-treated mice compared to anti-RANKL Ab-treated mice

We performed a longitudinal BLI to assess whether the antiresorptive agents tested here had an effect on bacterial load (Figure 3A). The bioluminescent signal peaked on Day 3 in all groups, and gradually became attenuated in the Ctl and anti-RANKL Ab groups, but attenuation was prolonged (Days 14–21) in the ZA group (Figure 3B). A two-way analysis of variance for repeated measurements showed a significant time effect [$F(2.331, 48.95) = 15.30$, $p < .0001$] and a significant treatment effect [$F(2.21) = 4.304$, $p = .0271$], but there was no time × treatment interaction effect [$F(6, 63) = 0.7727$, $p = .5942$]. There was no significant difference in bioluminescence intensity between the anti-RANKL Ab and Ctl groups at any time point, but it was significantly higher in the ZA group than in the Ctl group on Day 21 ($p = .0429$, Ctl vs. ZA; $1.23 \times 10^4 \pm 4.19 \times 10^4$ photons/s vs. $1.88 \times 10^6 \pm 8.66 \times 10^5$ photons/s).

3.3 | Differential effects of ZA and the anti-RANKL Ab on osteoclast formation and necrotic bone in osteomyelitis

The infected femora were histopathologically analyzed to investigate the effects of the antiresorptive agents on bone necrosis, bacterial nidus, and osteoclast formation (Figure 4A). Anti-RANKL Ab-treated mice did not show an increased amount of necrotic bone compared to Ctl mice, whereas ZA-treated mice had large amounts of non-resorbed necrotic bone, as evidenced by the presence of empty lacunae, at the distal metaphyseal region of the infected femur. The ratio of empty bone lacunae was significantly higher in the ZA group than in the other groups (ZA vs. Ctl: $p = .0489$, ZA vs. anti-RANKL Ab: $p = .0299$; Figure 4B). In addition, necrotic bone served as a nidus for infection as evidenced by a significantly higher semiquantitative Gram stain score (Figure 4C) and a larger number of gram-positive cocci (Figure 4A) in the necrotic bone of ZA-treated mice compared with the Ctl group. We next examined the number of osteoclasts and their distribution in the distal metaphyseal region of the femur, where infectious osteolysis occurred (Figure 5A). TRAP staining of histological sections of the femur showed that bacterial infection induced a large number of osteoclasts in the Ctl mice, while ZA-treated mice showed a remarkable reduction in the number of osteoclasts. Although anti-RANKL Ab treatment also reduced osteoclast numbers, it is noteworthy that osteoclasts accumulated on the surface of the necrotic bone in the anti-RANKL Ab-treated mice. To quantitatively evaluate the difference in the distribution pattern of osteoclasts, we separately measured the number of osteoclasts on the surfaces of live bone and necrotic bone (Figure 5A,B). As compared to Ctl, anti-RANKL Ab treatment, similar to ZA treatment, significantly reduced N.Oc/BS, Oc.S/BS, and ES/BS in live bone. On the other hand, in necrotic bone, anti-RANKL Ab treatment reduced osteoclast number, but its effect was significantly lesser than that of ZA. These histological findings suggest that osteoclast formation in the necrotic bone is RANKL-independent.

3.4 | IL-1β and TNF-α-induced osteoclast differentiation is not inhibited by the anti-RANKL Ab in vitro

To substantiate the histological findings of an intense inflammatory response around the necrotic bone-induced osteoclasts in the

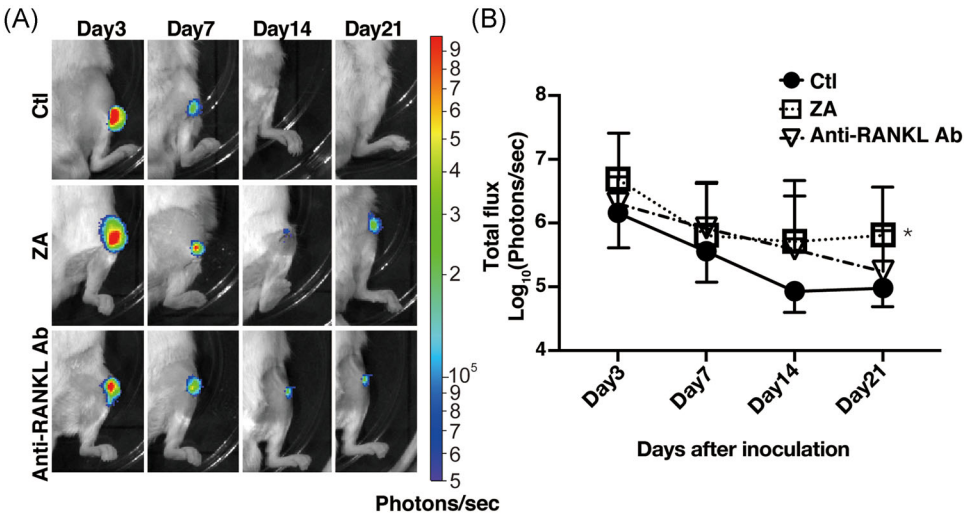

FIGURE 3 Time course of changes in bacterial load in a murine model of osteomyelitis in each treatment group. *Staphylococcus aureus* strain Xen 29 was inoculated into the left femur of the mice and treated with phosphate-buffered saline (PBS), zoledronic acid, or anti-RANKL monoclonal antibody. (A) The bacterial photon intensity of the left femur was sequentially measured on Days 3, 7, 14, and 21 after bacterial inoculation. (B) Line graphs showing photon counts for the region of interest in each treatment group ($n = 8$) at different time points. Values shown are mean ± *SEM* (*$p < .05$; vs. Ctl). Ctl, control [Color figure can be viewed at wileyonlinelibrary.com]

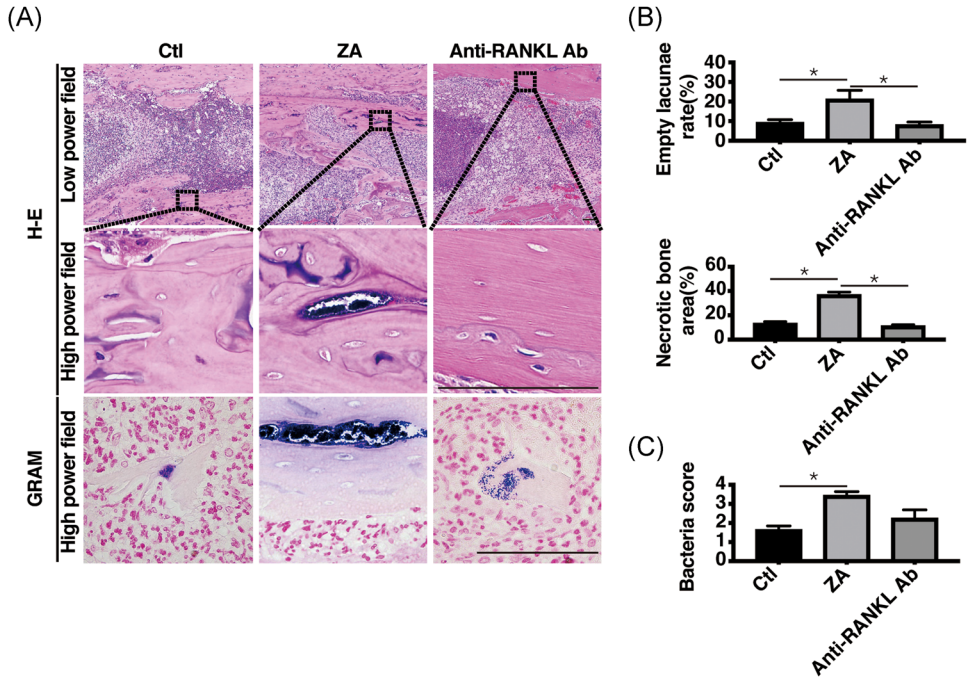

FIGURE 4 Histological analysis to investigate the changes induced by osteomyelitis in each treatment group. (A) Representative histological images of the bacterial inoculation site in the left femur on Day 21 after bacterial inoculation, in each treatment group. The first row shows the results of the hematoxylin and eosin staining (H&E) in a low-power field. The second row shows a magnified image of the region marked by the dashed square in the first row. The third row shows the magnified histology of Gram staining. Space, where the Gram-stain positive bacteria aggregated, was the haversian canal in the necrotic bone in ZA-treated mice. Scale bar = 100 μm. (B) The upper bar graph shows the ratio of empty lacunae measured from the H&E sections from each group ($n = 5$). The lower bar graph shows the ratio of necrotic bone area to total bone area ($n = 5$). (C) Bar graph showing the semiquantitative score for bacterial counts in each treatment group ($n = 5$); Ctl: control group; ZA: zoledronic acid treatment group; Anti-RANKL: anti-mouse RANKL monoclonal antibody treatment group. Values shown are mean ± *SEM* (*$p < .05$) [Color figure can be viewed at wileyonlinelibrary.com]

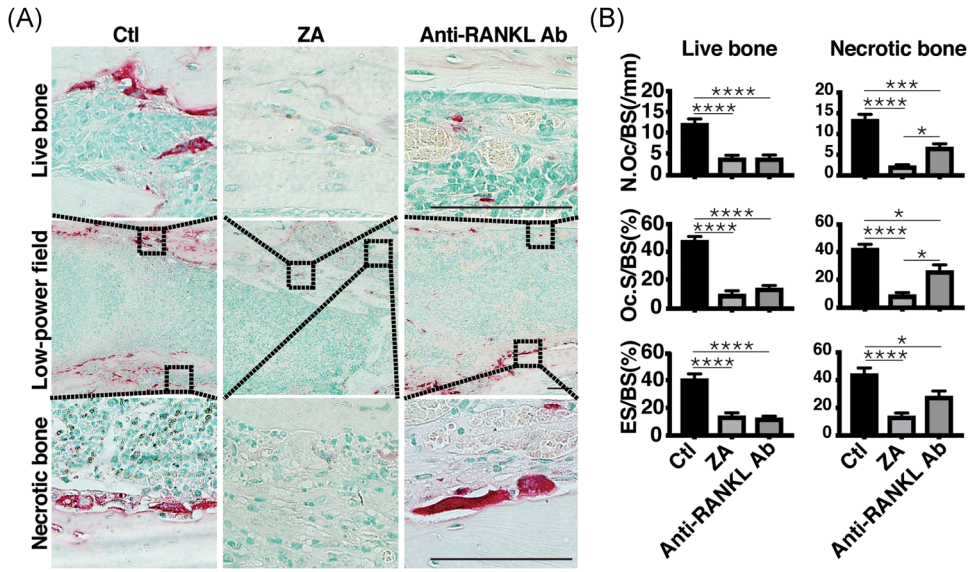

FIGURE 5 Histological analysis of the osteoclast development and activity in each treatment group. (A) Representative TRAP-stained histological sections of infected femurs on Day 21 after bacterial inoculation. The images in the middle row show the low-power field results. The upper row shows a magnified image of the region marked by the dashed square in the middle row, as the area on live bone. The images in the lower row show a magnified image of the region marked by the dashed square in the middle row, as the area on necrotic bone. Scale bar = 100 μm.
(B) Comparisons of osteoclast number (N.Oc/BS), osteoclast surface (Oc.S/BS), and eroded surface (ES/BS) on live bone and necrotic bone, respectively. Values shown are mean ± *SEM* (*$p < .05$, **$p < .01$, ***$p < .001$, ****$p < .0001$) [Color figure can be viewed at wileyonlinelibrary.com]

presence of anti-RANKL Ab, we performed an in vitro osteoclast differentiation assay under conditions simulating osteomyelitis (Figure 6). A coculture of BMMs and BMSCs that express RANKL mimics a live bone environment. A monoculture of BMMs mimics a necrotic bone environment. To simulate inflammatory conditions, we added the proinflammatory cytokines IL-1β and TNF-α to the cell culture medium. First, we evaluated the dose-dependent effect of ZA and anti-RANKL Ab on inflammatory cytokine-induced RANKL-dependent osteoclast differentiation, referring to previous reports[21,26] (Figure 6A). ZA showed a dose-dependent inhibitory effect on osteoclast induction from 0.001 to 1 μM. Anti-RANKL Ab also showed a dose-dependent inhibitory effect on osteoclast induction and a concentration of 0.1 μg/ml resulted in a ceiling effect. The anti-RANKL Ab at a concentration of 1 μg/ml markedly inhibited osteoclastogenesis under coculture conditions, mildly suppressed osteoclastogenesis in the coculture medium supplemented with IL-1β and TNF-α, and did not suppress osteoclastogenesis in the monoculture medium supplemented with IL-1β and TNF-α (Figure 6B,C).

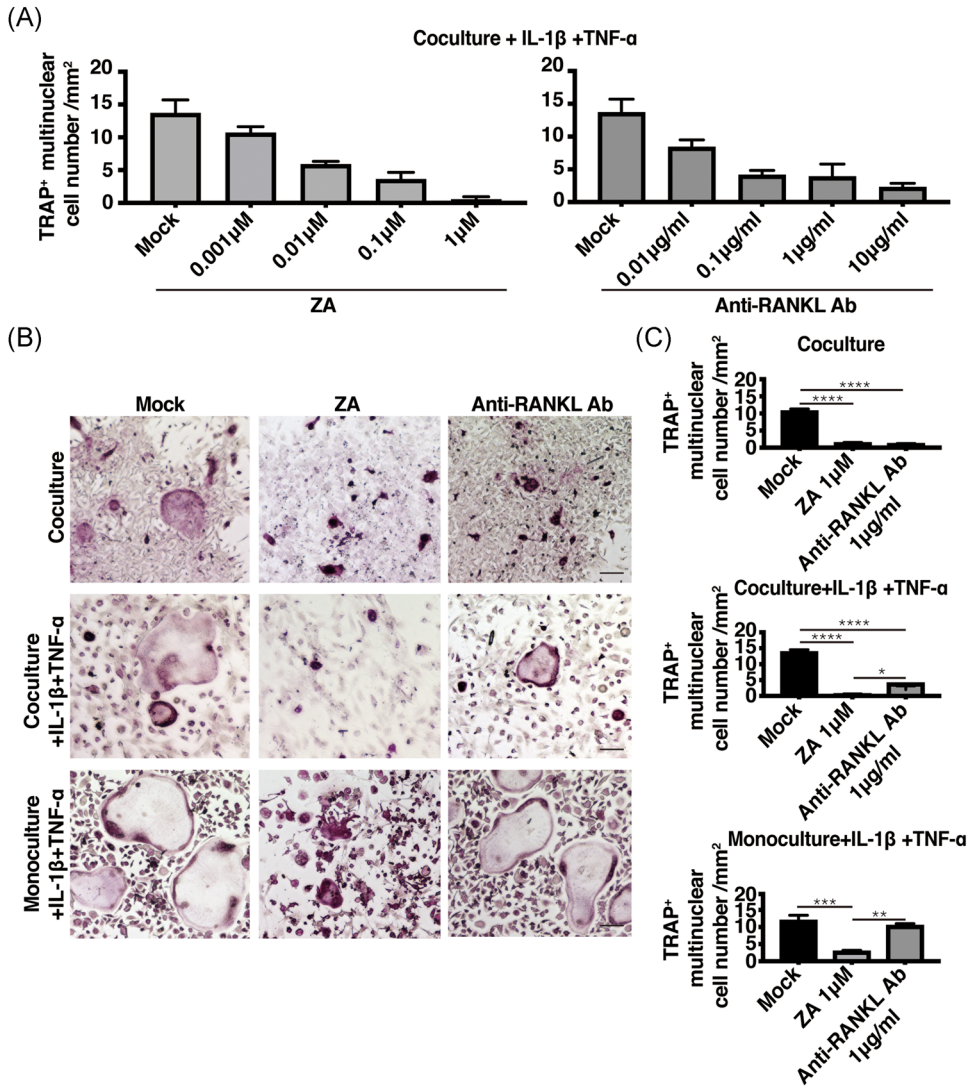

FIGURE 6 In vitro osteoclastogenesis assay to examine the effect of each treatment on inflammatory cytokine-induced RANKL-dependent or independent osteoclast differentiation. (A) Dose-dependent effect of ZA and anti-RANKL Ab on inflammatory cytokine-induced RANKL-dependent osteoclast differentiation ($n = 5$ for each dose). (B) Representative images of in vitro osteoclastogenesis assay. Bone marrow macrophages (BMMs) were monocultured in the presence of M-CSF. BMMs were cocultured with bone marrow stromal cells (BMSC) in the presence of 1, 25-dihydroxyvitamin D3 and M-CSF. The control group was administered phosphate-buffered saline, the ZA group was administered ZA, and the anti-RANKL Ab group was administered the anti-RANKL Ab. Images in the upper row show the coculture on Day 5, which simulated normal live bone. Images in the middle row show the coculture in the presence of IL-1β and TNF-α, which simulated live bone with the inflammation seen in osteomyelitis. Images in the lower row show the monoculture in the presence of IL-1β and TNF-α, which simulated necrotic bone with inflammation in osteomyelitis. Scale bar = 100 μm. (C) The number of TRAP-positive multinuclear cells in each culture condition in each treatment group ($n = 5$). Values shown are mean ± *SEM* (*$p < .05$, **$p < .01$, ***$p < .001$, ****$p < .0001$). IL, interleukin; M-CSF, macrophage colony-stimulating factor; RANKL, receptor activator of nuclear factor-kB ligand; TNF-α, tumor necrosis factor-α; ZA, zoledronic acid [Color figure can be viewed at wileyonlinelibrary.com]

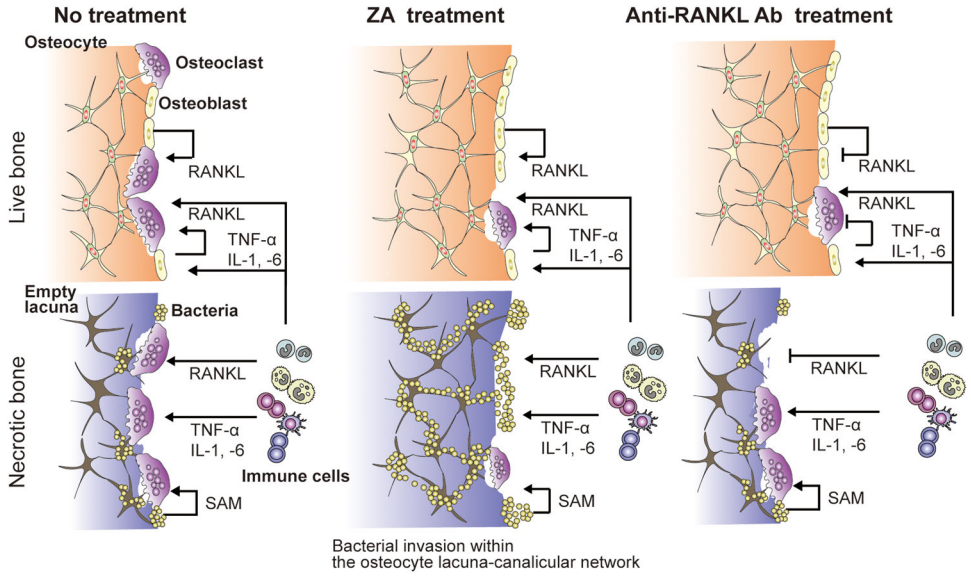

FIGURE 7 Schematic representation of the mechanism of action of zoledronic acid (ZA) and the anti-RANKL Ab for osteomyelitis. Bacterial infection promotes bone resorption of both live bone and necrotic bone through an increase in the expression of inflammatory cytokines, such as tumor necrosis factor-α (TNF-α), interleukin-1 (IL-1), and IL-6 as well as receptor activator of nuclear factor-kappa B ligand (RANKL) from osteoblasts and infiltrated immune cells and through *S. aureus* surface-associated material (SAM). Osteoblasts and osteocytes, which are the sources of RANKL, undergo apoptosis within the necrotic bone. ZA treatment induces apoptosis of osteoclasts in both live bone and necrotic bone, leading to an increase in necrotic bone, which harbors bacteria within the osteocyte lacuna-canalicular system. In contrast, anti-RANKL Ab treatment suppresses RANKL-dependent osteoclast differentiation of live bone but does not suppress RANKL-independent bone resorption induced by inflammatory cytokines and SAM [Color figure can be viewed at wileyonlinelibrary.com]

ZA at a concentration of 1 μM suppressed osteoclast differentiation under both coculture and monoculture conditions (Figure 6B,C). These results suggest that the anti-RANKL Ab does not effectively block osteoclast formation at the site of intense inflammation.

4 | DISCUSSION

Despite the potential benefits of antiresorptive therapy against rapidly progressive osteolysis caused by bacterial infection, preclinical data from previous animal studies suggest it has adverse effects on necrotic bone.[12,13] Consistent with previous reports, the histological findings of this study revealed that ZA facilitated the accumulation of necrotic bone, which served as a nidus for infection, while an anti-RANKL Ab did not inhibit the osteoclastic removal of the necrotic bone in a murine model of osteomyelitis. The difference in the effect on the necrotic bone between these two drugs can be explained by RANKL-independent osteoclast formation around the necrotic bone in mice treated with an anti-RANKL Ab. Osteoclast formation is induced by osteoblasts, osteocytes, and polymorphonuclear cells through the induction of RANKL, which can be blocked by the anti-RANKL Ab. However, there is another contributor to osteoclastogenesis and bone resorptive activity in osteomyelitis. Staphylococcal infection is associated with elevated levels of proinflammatory cytokines, such as TNF-α and IL-1β, which can directly induce osteoclast formation via a RANKL-independent mechanism.[6,16–18] Therefore, although anti-RANKL Ab may be inferior to BP in preserving bone stock it has advantages in removing necrotic bone in osteomyelitis.

While we do not want to overstate the implication of our findings that the anti-RANKL Ab did not significantly increase necrotic bone in osteomyelitis, the great need for better treatments for patients with osteomyelitis may reinvigorate the research on antiresorptive therapies against osteomyelitis. Bacterial invasion within the osteocyte lacuna-canalicular network of the necrotic bone, as well as biofilm formation on dead bone, is considered to be the cause of the chronicity of osteomyelitis.[27] Therefore, osteoclastic resorption of necrotic bone is considered to be a necessary process for healing in osteomyelitis and should not be suppressed by antiresorptive therapy. Given that osteoblasts and osteocytes undergo apoptosis in the necrotic bone and therefore are no longer sources of RANKL, inflammatory cytokines and toxic factors such as SAM rather than RANKL play essential roles in removing necrotic bone (Figure 7). If this is the case, then anti-RANKL therapy could exert an osteoprotective effect on live bone and the least adverse effect on the removal of necrotic bone.

It should be noted that denosumab, a human anti-RANKL Ab, has been demonstrated to reduce inflammatory joint bone erosion in patients with RA in phase II clinical trials, suggesting the importance of RANKL/RANK signaling as a critical inducer of inflammatory bone destruction.[11] However, given that the participants in this study all received methotrexate therapy, it is possible that inflammatory cytokines suppressed to levels that were too low to induce osteoclasts in a RANKL-independent manner. Furthermore, O'Brien et al.[28]

demonstrated that in the absence of RANK, mice still developed bone erosions and bone-resorbing functional osteoclasts in inflamed joints using K/BxN serum-transfer arthritis model mice with a conditional deletion of RANK. This study clearly demonstrates that RANK signaling is not an absolute requirement for inflammatory bone destruction and that a variety of inflammatory cytokines contribute to the generation of osteoclasts at the inflammatory site. In cases of infectious osteomyelitis, intense inflammation occurs in response to bacterial infection, and the use of immunosuppressants is contraindicated as it may exacerbate the infection. These facts support our findings that an anti-RANKL Ab did not suppress osteoclast formation and the resorption of necrotic bone, at the site of intense inflammation in osteomyelitis.

This study has several limitations. First, we did not administer antibiotics to mice with osteomyelitis despite the fact that it is a standard treatment for osteomyelitis in clinical practice. This is because in our *S. aureus* inoculation model of osteomyelitis the infection is spontaneously resolved by Day 21 after inoculation, as evidenced by the attenuation of the bioluminescent signal seen during the longitudinal BLI observation. Second, although an observation period of 21 days is sufficient to study the effects of antiresorptive therapies on progressive osteolysis during the active infection phase it is not long enough to study their effects on bone regeneration and remodeling in the subsequent reparative phase. Further experiments with a longer observation period should be performed in future studies. Third, we did not analyze the effect of antiresorptive therapies on immunity. However, an earlier study demonstrated that antiresorptive agents, including alendronate and osteoprotegerin, had no remarkable effect on humoral immunity.[12] Fourth, our findings on the effect of the anti-RANKL Ab on necrotic bone may only be applicable to osteomyelitis caused by virulent bacteria, such as *S. aureus*, which cause a robust inflammatory response. In the case of osteomyelitis caused by less virulent bacteria, which cause mild inflammation, the resorption of necrotic bone may not occur following treatment with an anti-RANKL Ab, as is seen with ZA.

In conclusion, our work demonstrates that anti-RANKL Ab may exert an osteoprotective effect without hampering the removal of the necrotic bone, which serves as a nidus for infection in osteomyelitis.

ACKNOWLEDGMENTS

This work was supported by the Japan Society for the Promotion of Science (JSPS) Grants-in-Aid for Scientific Research (KAKENHI) (Grant Number: JP17H04309).

CONFLICT OF INTERESTS

The authors declare that there are no conflict of interests.

AUTHOR CONTRIBUTIONS

Hideyuki Kobayashi: contributed to research design, data acquisition, analysis and interpretation of data, and drafting of the paper. **Ryo Fujita:** contributed to data acquisition, analysis and interpretation of data, and drafting of the paper. **Shigeto Hiratsuka:** contributed to research design, data acquisition, analysis and interpretation of data. **Tomohiro Shimizu:** contributed to data acquisition. **Dai Sato:** contributed to data acquisition. **Hiroki Hamano:** contributed to data acquisition. **Norimasa Iwasaki:** contributed to interpretation of data. **Masahiko Takahata:** contributed to research design, interpretation of data, and drafting and critically revising the paper. All authors have read and approved the final submitted manuscript.

ORCID

Masahiko Takahata http://orcid.org/0000-0002-2436-2175

REFERENCES

1. Simpson AHRW, Deakin M, Latham JM. Chronic osteomyelitis: the effect of the extent of surgical resection on infection-free survival. *J Bone Joint Surg Br*. 2001;83-B:403-407.
2. Reichert JC, Saifzadeh S, Wullschleger ME, et al. The challenge of establishing preclinical models for segmental bone defect research. *Biomaterials*. 2009;30:2149-2163.
3. Perry CR. Bone repair techniques, bone graft, and bone graft substitutes. *Clin Orthop Relat Res*. 1999;360:71-86.
4. Garrido-Gómez J, Arrabal-Polo MA, Girón-Prieto MS, Cabello-Salas J, Torres-Barroso J, Parra-Ruiz J. Descriptive analysis of the economic costs of periprosthetic joint infection of the knee for the public health system of Andalusia. *J Arthroplasty*. 2013;28:1057-1060.
5. Mackowiak PA, Jones SR, Smith JW. Diagnostic value of sinus-tract cultures in chronic osteomyelitis. *JAMA*. 1978;239:2772-2775.
6. Lau YS, Wang W, Sabokbar A, et al. Staphylococcus aureus capsular material promotes osteoclast formation. *Injury*. 2006;37:S41-S48.
7. Yoshii T, Magara S, Miyai D, et al. Local levels of interleukin-1β, -4, -6, and tumor necrosis factor α in an experimental model of murine osteomyelitis due to staphylococcus aureus. *Cytokine*. 2002;19:59-65.
8. Pfeilschifter J, Chenu C, Bird A, Mundy GR, Roodman GD. Interleukin-1 and tumor necrosis factor stimulate the formation of human osteoclastlike cells in vitro. *J Bone Miner Res*. 1989;4:113-118.
9. Ishimi Y, Miyaura C, Jin CH, et al. IL-6 is produced by osteoblasts and induces bone resorption. *J Immun*. 1990;145:3297-3303.
10. Jarrett SJ, Conaghan PG, Sloan VS, et al. Preliminary evidence for a structural benefit of the new bisphosphonate zoledronic acid in early rheumatoid arthritis. *Arthritis Rheum*. 2006;54:1410-1414.
11. Cohen SB, Dore RK, Lane NE, et al. Denosumab treatment effects on structural damage, bone mineral density, and bone turnover in rheumatoid arthritis: a twelve-month, multicenter, randomized, double-blind, placebo-controlled, phase II clinical trial. *Arthritis Rheum*. 2008;58:1299-1309.
12. Li D, Gromov K, Proulx ST, et al. Effects of antiresorptive agents on osteomyelitis: novel insights on osteonecrosis of the jaw (ONJ) pathogenesis. *Ann N Y Acad Sci*. 2010;1192:84-94.
13. Morita M, Iwasaki R, Sato Y, et al. Elevation of pro-inflammatory cytokine levels following anti-resorptive drug treatment is required for osteonecrosis development in infectious osteomyelitis. *Sci Rep*. 2017;7:46322.
14. Roelofs AJ, Thompson K, Gordon S, Rogers MJ. Molecular mechanisms of action of bisphosphonates: current status. *Clin Cancer Res*. 2006;12:6222s-6230s.
15. Lacey DL, Boyle WJ, Simonet WS, et al. Bench to bedside: elucidation of the OPG-RANK-RANKL pathway and the development of denosumab. *Nat Rev Drug Discov*. 2012;11:401-419.

16. Kudo O, Sabokbar A, Pocock A, Itonaga I, Fujikawa Y, Athanasou NA. Interleukin-6 and interleukin-11 support human osteoclast formation by a RANKL-independent mechanism. *Bone*. 2003;32:1-7.
17. Azuma Y, Kaji K, Katogi R, Takeshita S, Kudo A. Tumor necrosis factor-alpha induces differentiation of and bone resorption by osteoclasts. *J Biol Chem*. 2000;275:4858-4864.
18. Kobayashi K, Takahashi N, Jimi E, et al. Tumor necrosis factor α stimulates osteoclast differentiation by a mechanism independent of the Odf/Rankl–Rank interaction. *J Exp Med*. 2000;191:275-286.
19. Funao H, Ishii K, Nagai S, et al. Establishment of a real-time, quantitative, and reproducible mouse model of Staphylococcus osteomyelitis using bioluminescence imaging. *Infect Immun*. 2012;80:733-741.
20. Sims NA, Green JR, Glatt M, et al. Targeting osteoclasts with zoledronic acid prevents bone destruction in collagen-induced arthritis. *Arthritis Rheum*. 2004;50:2338-2346.
21. Furuya Y, Mori K, Ninomiya T, et al. Increased bone mass in mice after single injection of anti-receptor activator of nuclear factor-κB ligand-neutralizing antibody: evidence for bone anabolic effect of parathyroid hormone in mice with few osteoclasts. *J Biol Chem*. 2011;286:37023-37031.
22. Mirels H. Metastatic disease in long bones. A proposed scoring system for diagnosing impending pathologic fractures. *Clin Orthop Relat Res*. 1989;249:256-264.
23. Church D, Melnyk E, Unger B. Quantitative gram stain interpretation criteria used by microbiology laboratories in Alberta, Canada. *J Clin Microbiol*. 2000;38:4266-4268.
24. Takeshita S, Kaji K, Kudo A. Identification and characterization of the new osteoclast progenitor with macrophage phenotypes being able to differentiate into mature osteoclasts. *J Bone Miner Res*. 2000;15:1477-1488.
25. Peister A, Mellad JA, Larson BL, Hall BM, Gibson LF, Prockop DJ. Adult stem cells from bone marrow (MSCs) isolated from different strains of inbred mice vary in surface epitopes, rates of proliferation, and differentiation potential. *Blood*. 2004;103:1662-1668.
26. Sudhoff H, Jung JY, Ebmeyer J, Faddis BT, Hildmann H, Chole RA. Zoledronic acid inhibits osteoclastogenesis in vitro and in a mouse model of inflammatory osteolysis. *Ann Otol Rhinol Laryngol*. 2003;112:780-786.
27. de Mesy Bentley KL, Trombetta R, Nishitani K, et al. Evidence of Staphylococcus Aureus deformation, proliferation, and migration in canaliculi of live cortical bone in murine models of osteomyelitis. *J Bone Miner Res*. 2017;32:985-990.
28. O'Brien W, Fissel BM, Maeda Y, et al. RANK-Independent osteoclast formation and bone erosion in inflammatory arthritis. *Arthritis Rheum*. 2016;68:2889-2900.

How to cite this article: Kobayashi H, Fujita R, Hiratsuka S, et al. Differential effects of anti-RANKL monoclonal antibody and zoledronic acid on necrotic bone in a murine model of *Staphylococcus aureus*-induced osteomyelitis. *J Orthop Res*. 2021;1-10. https://doi.org/10.1002/jor.25102